

SUPPORTING FILE

A Self-Assembled Nanoprobe Based on Schiff Base for the Rapid and Selective Detection of Serum Albumin with Cell Imaging Applications

Dolan Moni,^a Mihir Sasmal^a, Abu Saleh Musha Islam^b, Ananya Dutta^a, Debjani Maiti^a, Rousunara Khatun^c, Atul Katarkar^d, Mahammad Ali^{a,*}

^aDepartment of Chemistry, Jadavpur University, Kolkata 700 032, India; E-mail: m_ali2062@yahoo.com

^bSchool of Chemical Sciences, Indian Association for the Cultivation of Science, 2A & 2B Raja S. C. Mullick Road, Kolkata 700032, India.

^cAliah University, II-A/27, Action Area II, Newtown, Action Area II, Kolkata, West Bengal 700160, India

^dDepartment of Biochemistry, University of Lausanne, Ch. des Boveresses 155, 1066 Epalinges, Switzerland.

No.	Content	Figure No.
1.	¹ H-NMR spectrum of NHC .	Fig. S1
2.	¹³ C-NMR spectrum of NHC .	Fig. S2
3.	Mass spectrum of NHC .	Fig. S3
4.	IR spectrum of NHC .	Fig. S4
5.	¹ H-NMR spectrum of DBNHC .	Fig. S5
6.	¹³ C-NMR spectra of DBNHC .	Fig. S6
7.	Mass spectrum of DBNHC .	Fig. S7
8.	IR spectrum of DBNHC .	Fig. S8
9.	UV-vis absorption and Fluorescence emission spectra of DBNHC in DMSO/PBS mixture.	Fig. S9
10.	Fluorescence responses of DBNHC towards BSA and various proteins.	Fig. S10
11.	Fluorescence responses of DBNHC towards BSA, various amino acids.	Fig. S11
12.	Fluorescence responses of DBNHC towards BSA, various anions and various cations.	Fig. S12
13.	Determination of detection limit of DBNHC for BSA	Fig. S13
14.	Time dependent fluorescent intensity changes of DBNHC , both in absence and presence of BSA.	Fig. S14
15.	Effects of pH on DBNHC for the detection of BSA.	Fig. S15
16.	Residuals plots of DBNHC both in absence and presence of BSA from the life time analysis experiment.	Fig. S16
17.	Fluorescence spectral change of DBNHC-BSA composite in presence of ibuprofen, hemin and warfarin.	Fig. S17

SUPPORTING FILE

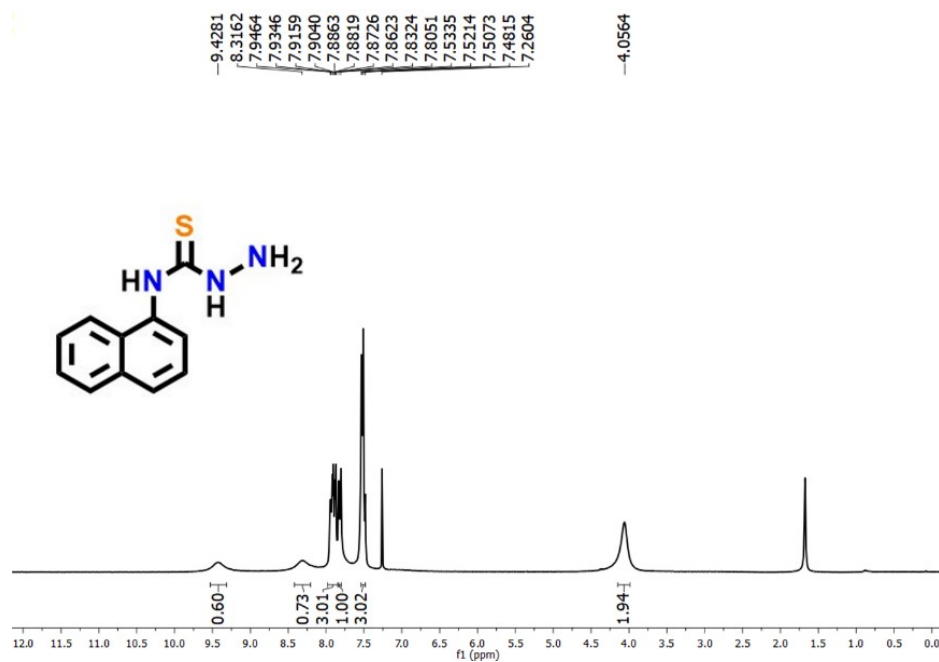


Fig. S1 ¹H-NMR spectrum of NHC in CDCl₃.

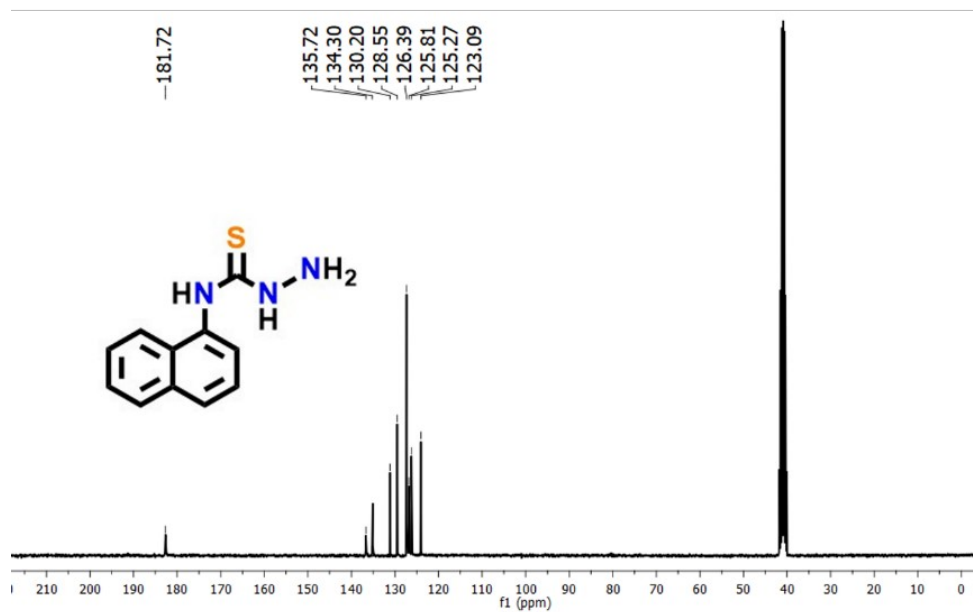


Fig. S2 ¹³C-NMR spectrum of NHC in DMSO-d₆.

SUPPORTING FILE

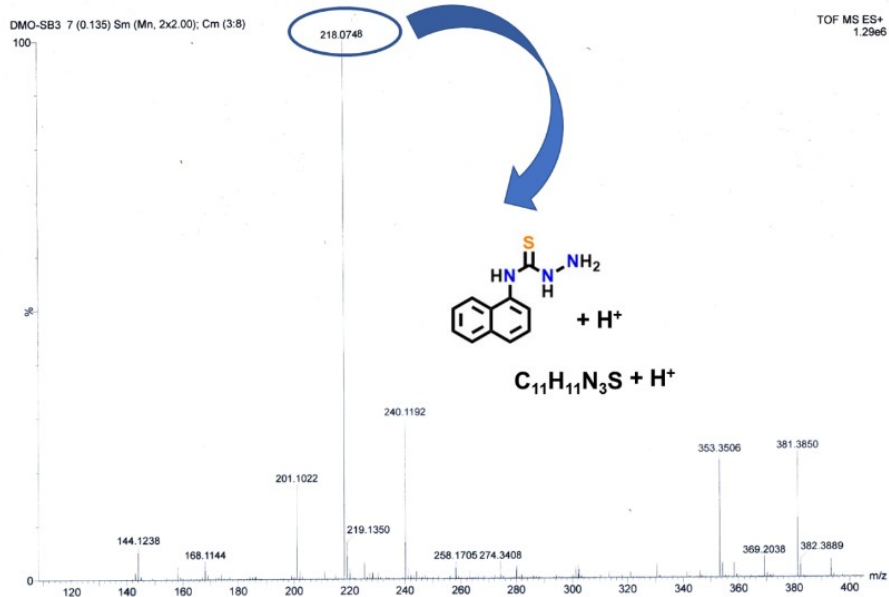


Fig. S3 Mass spectrum of NHC in MeOH.

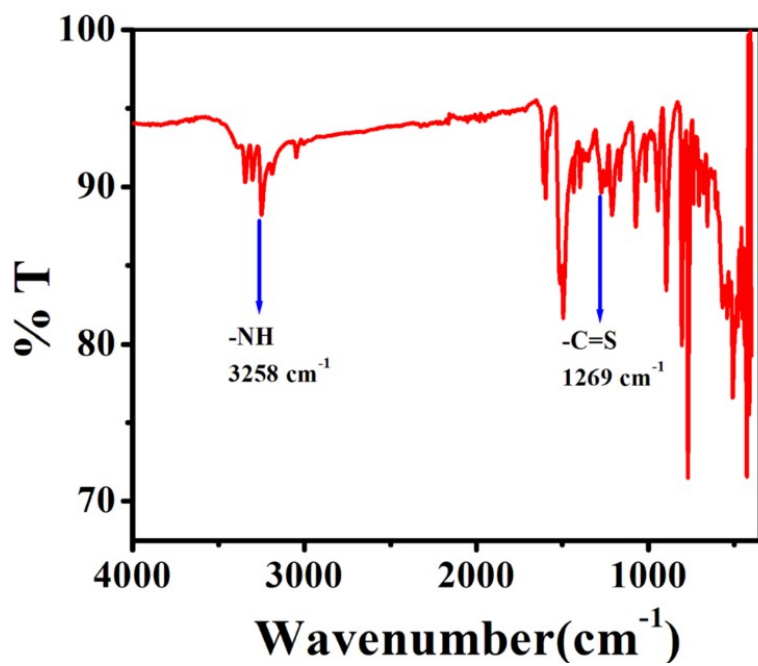


Fig. S4 IR spectrum of NHC.

SUPPORTING FILE

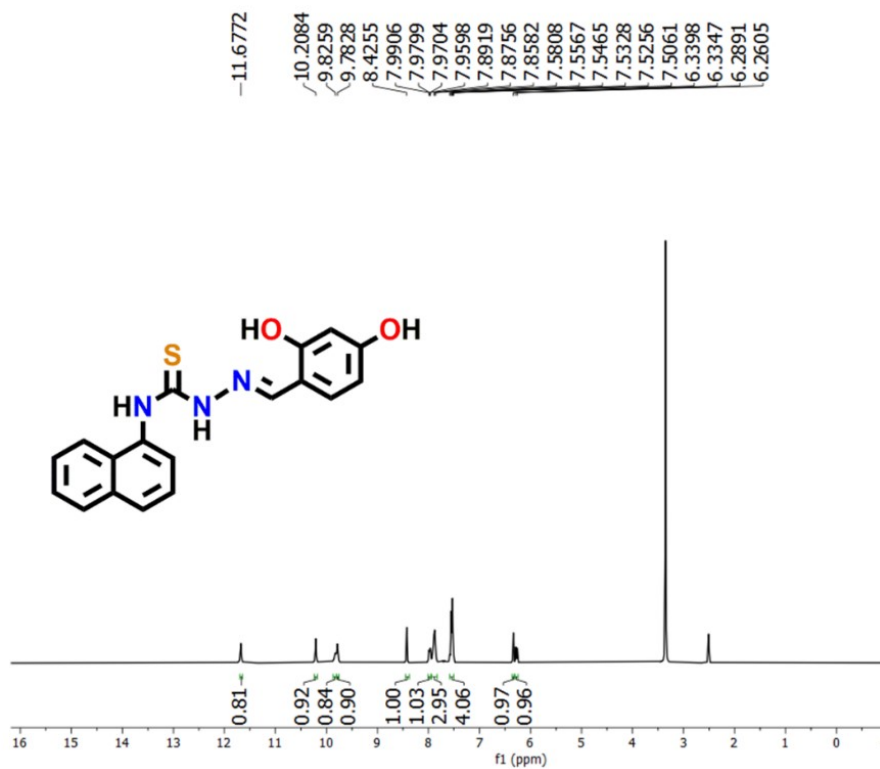


Fig. S5 ¹H-NMR spectrum of DBNHC in DMSO-d₆.

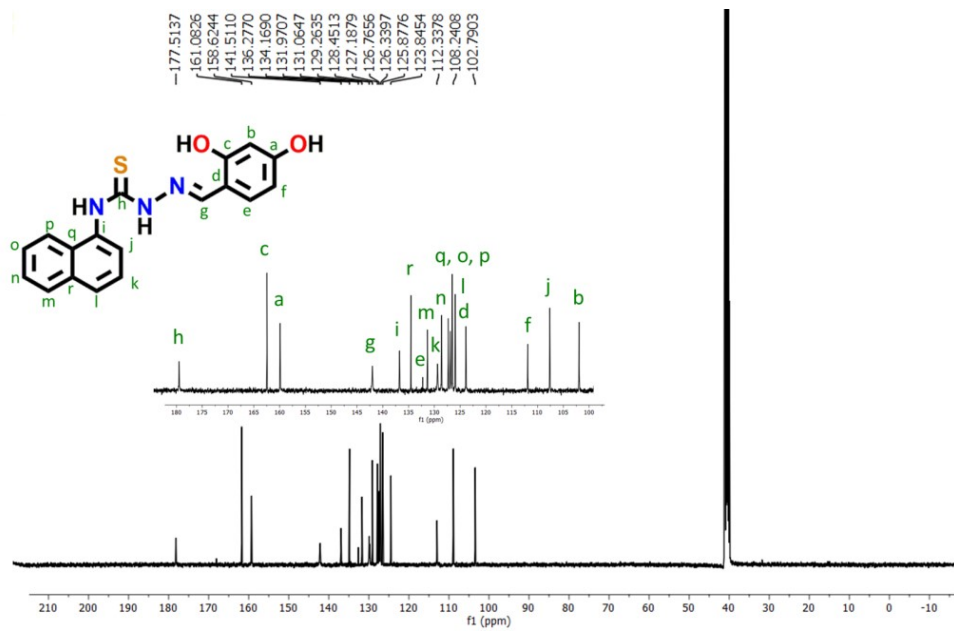


Fig. S6 ¹³C-NMR spectra of DBNHC in DMSO-d₆.

SUPPORTING FILE

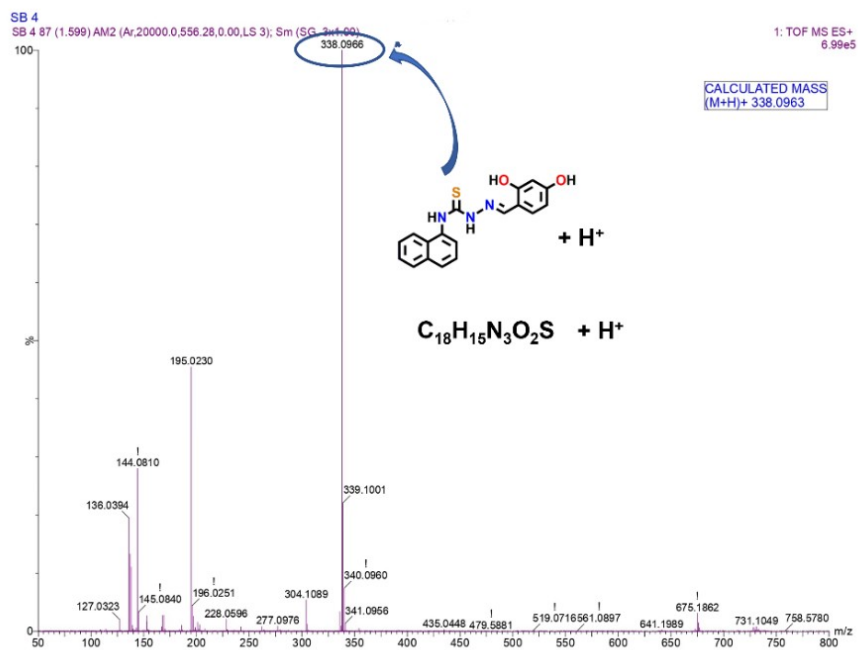


Fig. S7 Mass spectrum of DBNHC in MeOH.

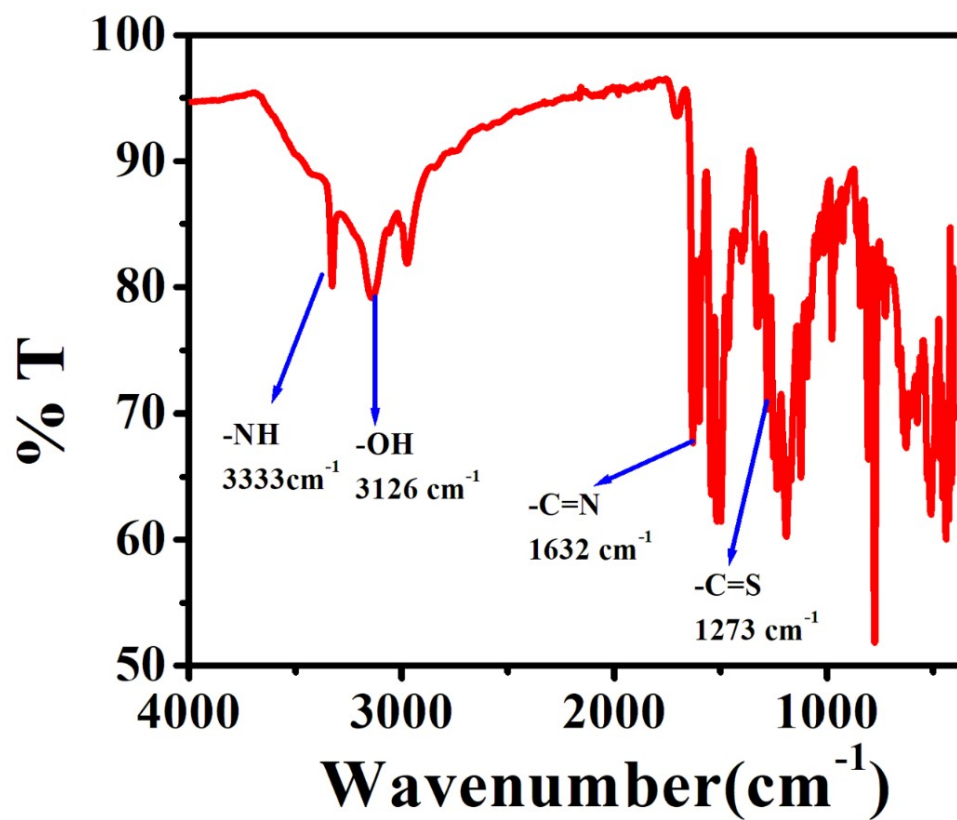


Fig. S8 IR spectrum of DBNHC.

SUPPORTING FILE

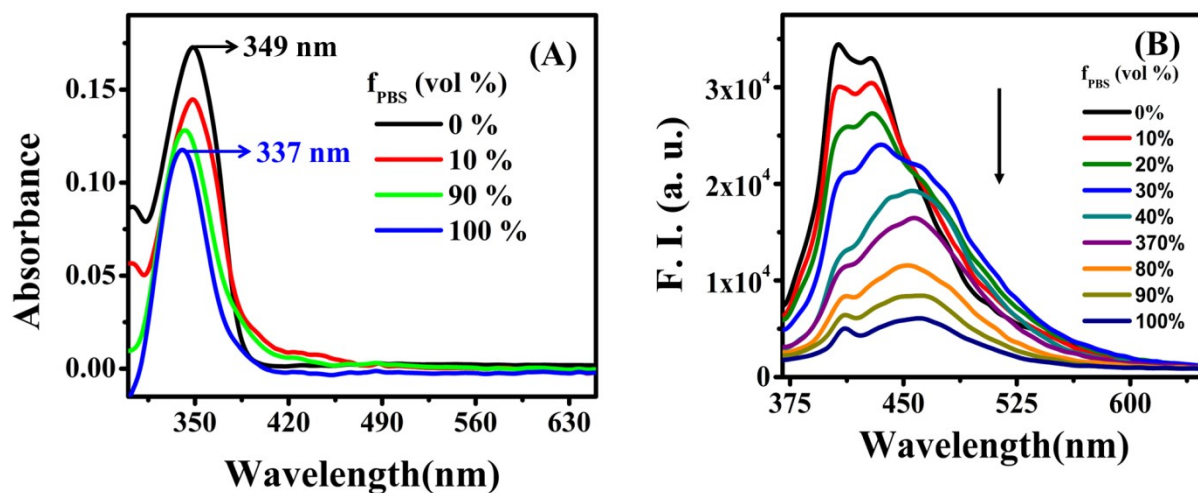


Fig. S9 (A) UV-vis absorption spectra of **DBNHC** ($5 \mu\text{M}$) in DMSO/PBS buffer mixtures with different PBS fractions (f_{PBS}). (B) Fluorescence emission spectra of **DBNHC** ($5 \mu\text{M}$) in DMSO/PBS buffer mixtures with different PBS fractions (f_{PBS}). $\lambda_{\text{ex}} = 355 \text{ nm}$.

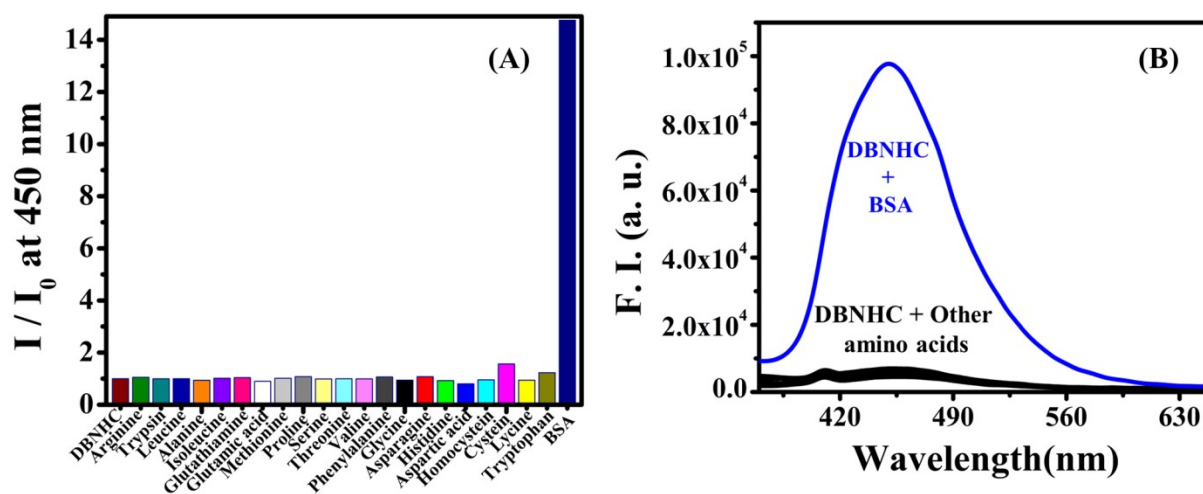


Fig. S10. Fluorescence responses of **DBNHC** ($5 \mu\text{M}$) at 450 nm ($\lambda_{\text{ex}} = 355 \text{ nm}$) towards **BSA** (8 equiv.) and various amino acids (8 equiv.) in $\sim 100\%$ PBS buffer pH 7.4 at room temperature. (B) Corresponding spectral responses of **DBNHC** towards different amino acids.

SUPPORTING FILE

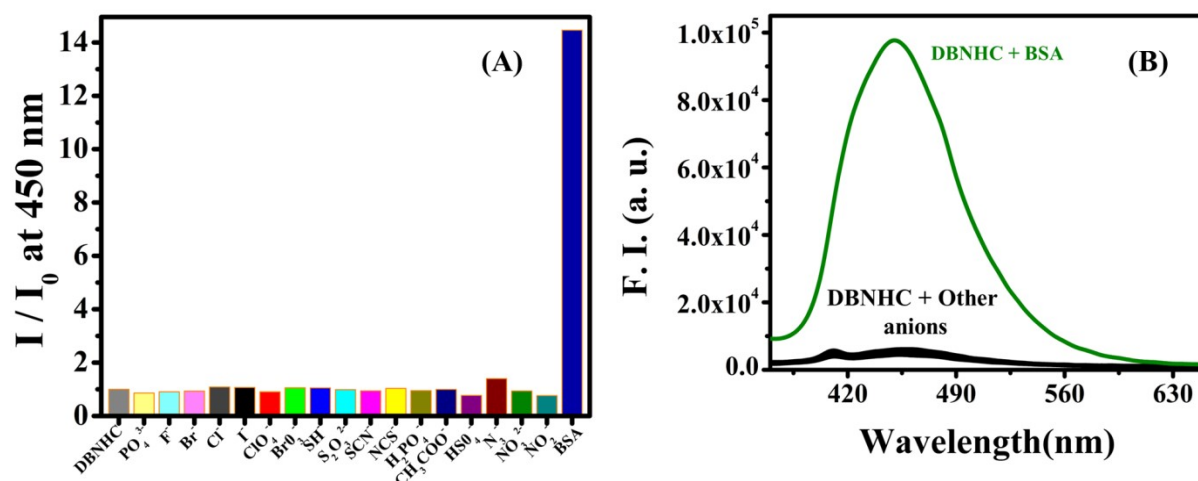


Fig. S11. (A) Fluorescence responses of **DBNHC** (5 μ M) towards **BSA** (8 equiv.) and various anions (12 equiv.) at 450 nm (λ_{ex} = 355 nm) in \sim 100% PBS buffer of pH 7.4. (B) Corresponding spectral responses of **DBNHC** towards different anions.

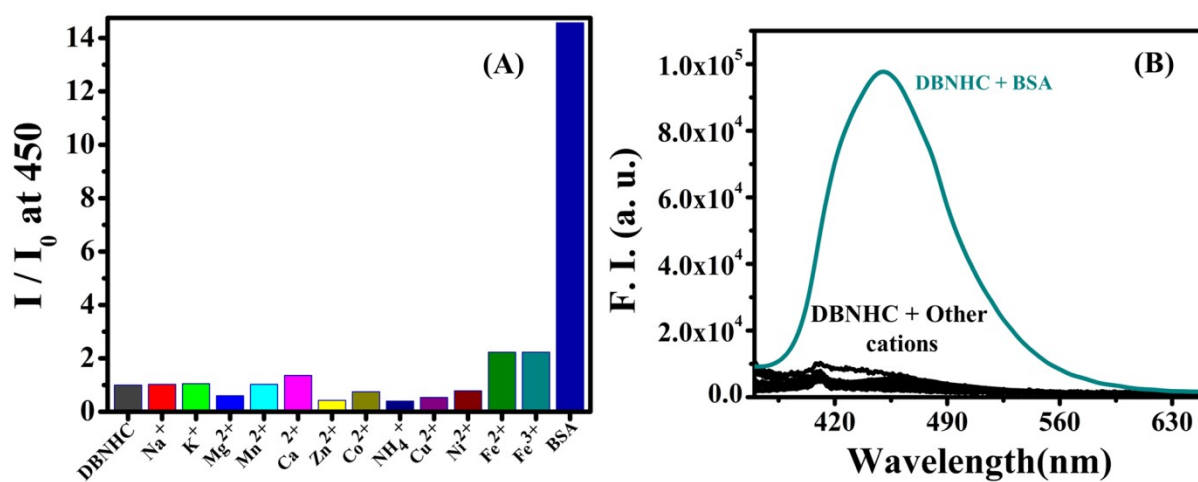


Fig. S12. Fluorescence responses of **DBNHC** (5 μ M) towards **BSA** (8 equiv.) and various cations (12 equiv.) at 450 nm (λ_{ex} = 355 nm) in \sim 100% PBS buffer of pH 7.4. (B) Corresponding spectral responses of **DBNHC** towards different cations.

SUPPORTING FILE

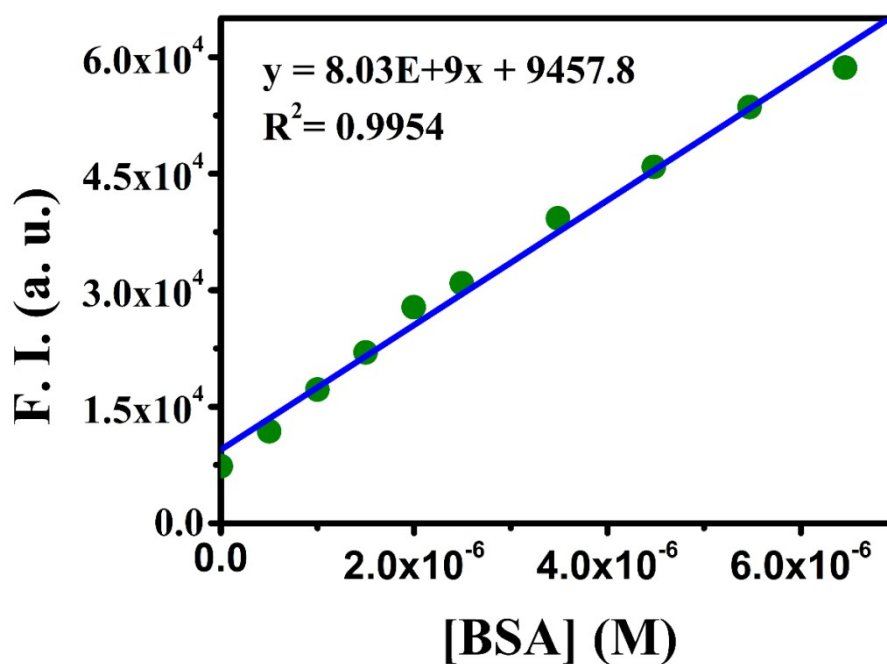


Fig. S13 Linear fluorescence response of DBNHC (5 μM) to BSA (0-6.46 μM) at 450 nm in ~100% PBS buffer of pH 7.4 for determination of detection limit. LOD value is estimated as 58 nM using formula $LOD = 3\sigma/slope$. The standard deviation, σ , of the blank (DBNHC only) was determined by measuring the fluorescence intensity 10 times separately at a fixed concentration of 5 μM using standard formula and was estimated to be 155.025. From the above graph we get slope (S) = $8.03 \times 10^9 M^{-1}$.

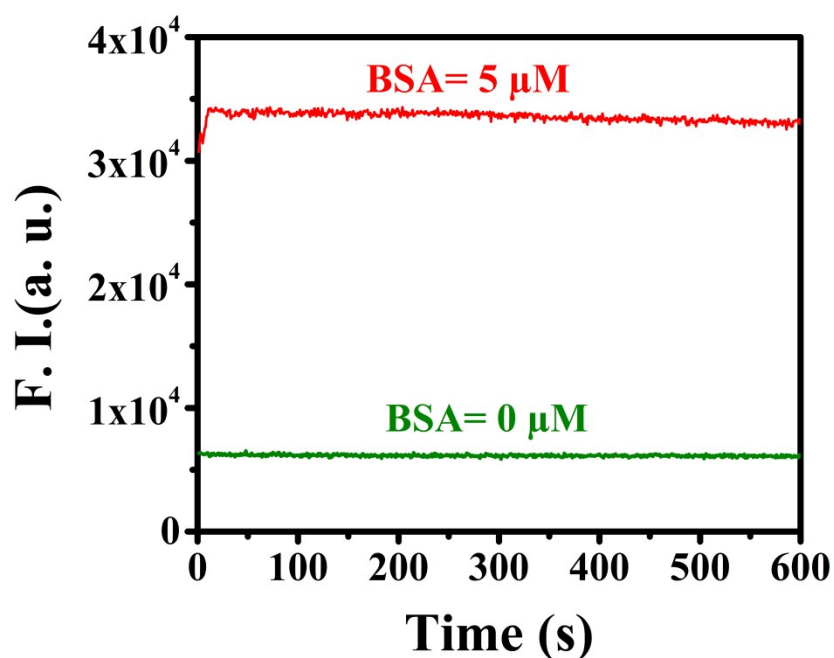


Fig. S14 Time dependent fluorescent intensity changes at 450 nm of DBNHC (5 μM) in the presence of 5 μM of BSA in ~100% PBS buffer of pH 7.4.

SUPPORTING FILE

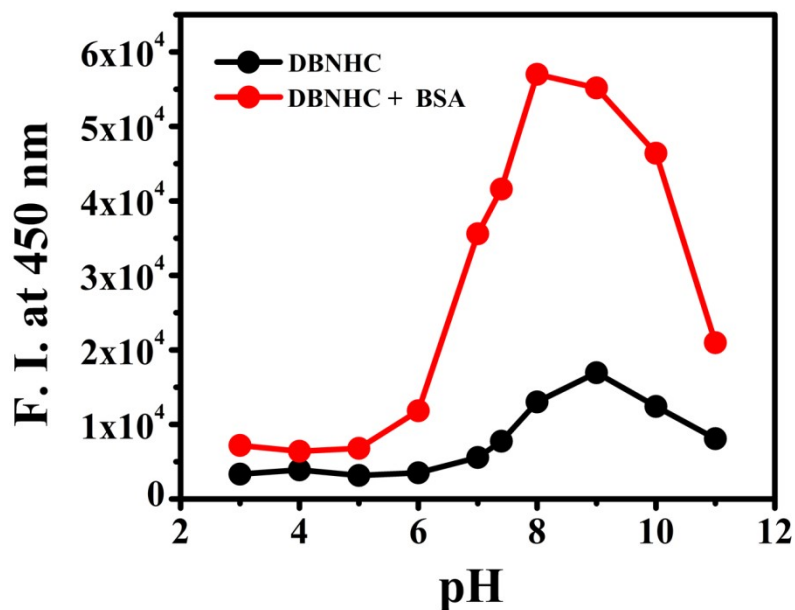


Fig. S15 The fluorescence emission intensities of **DBNHC** (5 μM) at 450 nm in the absence and presence of **BSA** (1 equiv.) at different pH. All the experiments were performed in PBS buffer. $\lambda_{\text{ex}} = 355 \text{ nm}$.

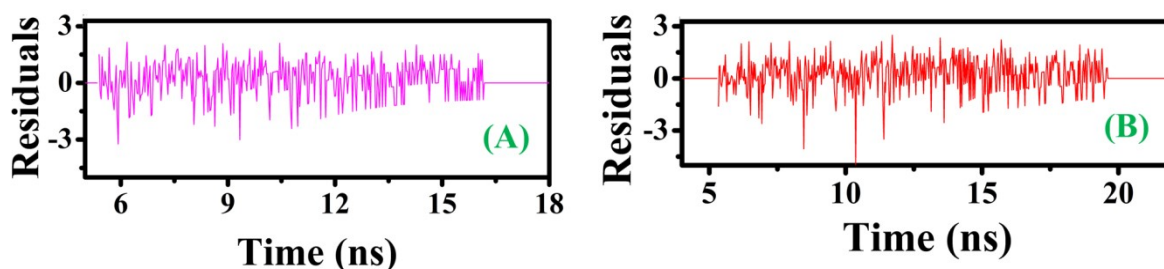


Fig. S16 Residuals plots of (A) **DBNHC** (5 μM) only (B) **DBNHC** in presence of **BSA** from the life time analysis experiment.

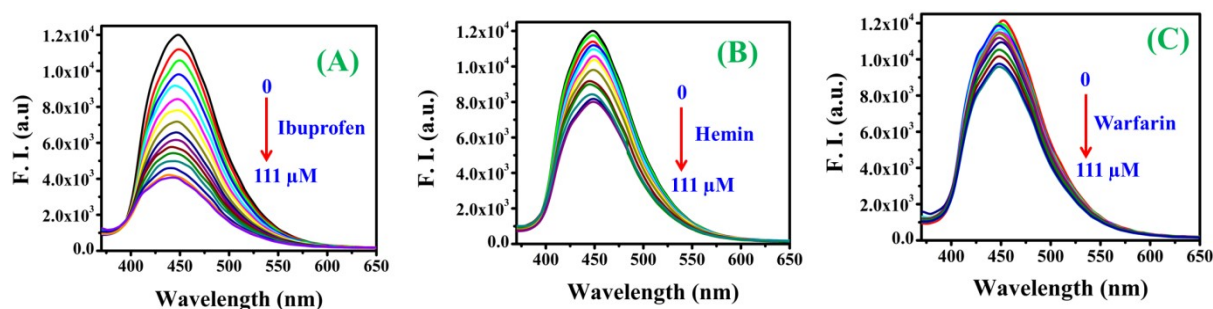


Fig. S17 Fluorescence spectral change of **DBNHC-BSA** composite (**DBNHC** = 5 μM , **BSA** = 1.25 μM) in pH 7.4 PBS buffer with the successive addition of (A) **ibuprofen** (B) **hemin** (C) **warfarin** site markers (0–111 μM). $\lambda_{\text{ex}} = 355 \text{ nm}$.

Instrumentation

The ^1H NMR and ^{13}C NMR spectra were recorded on a Bruker 300 and 400 MHz spectrophotometer using tetramethylsilane as internal standard in CDCl_3 and $\text{DMSO}-d_6$. The following abbreviations were used to explain multiplicities: s = singlet, d = doublet, m = multiplet. The ESI- MS^+ (m/z) spectra of the probe was recorded on a HRMS spectrophotometer (model: QTOF Micro YA263). The Fourier transform infrared spectra ($4000\text{--}400 \text{ cm}^{-1}$) of the probe was recorded on a Perkin-Elmer RX I FT-IR spectrophotometer with a solid KBr disc. The UV-Vis absorbance spectral studies were carried out on an Agilent diode-array Spectrophotometer (Agilent 8453) using a 1 cm path length quartz cuvette in the wavelength range of 190-900

SUPPORTING FILE

nm. Steady-state fluorescence spectroscopic measurements were performed on a PTI spectrofluorimeter (Model QM-40) by using a fluorescence free quartz cuvette of 1 cm path length. The excitation and emission slit widths were fixed at 3 nm. Fluorescence lifetimes were determined from time-resolved intensity decay by the method of time correlated single photon counting (TCSPC) measurements using a picosecond diode laser (IBH Nanoled-07) in an IBH fluorocube apparatus. The fluorescence decay data were collected on a Hamamatsu MCP photomultiplier (R3809) and examined by the IBH DAS6 software.

UV-Vis and fluorescence spectroscopic studies

For various spectroscopic studies a stock solution of **DBNHC** (1×10^{-3} M) was prepared in DMSO from which 10 μ L was added to 2 mL of PBS buffer solution of pH 7.4 to get final concentration of 5 μ M. In the fluorescence selectivity experiment, the test samples were prepared by adding the appropriate volume of the stock solutions of the respective proteins, enzymes, metal ions, anions and other analytes into 2 mL solution of the probe **DBNHC** (5 μ M). For the fluorescence-titration experiments, another set of BSA standard solution (1×10^{-3} M) was prepared by diluting the earlier prepared 25 mg/mL stock solution in PBS medium. For the fluorescence-titration Quartz cuvette was filled with 2 mL of PBS buffer containing 5 μ M **DBNHC**, to which the newly prepared stock solutions of BSA (1×10^{-3} M) were gradually added using a micropipette as required. For the fluorescence experiments, excitation wavelength was set at 355 nm and emission were recorded from 365 to 650 nm. For the UV-Vis studies the probe concentration was also kept fixed at 5 μ M and the spectra were collected with proper background correction. For the competitive fluorescence binding experiments, stock solutions of warfarin and ibuprofen (1 mM for each) were prepared in deionized water and DMSO, respectively. In a typical assay, BSA solution was premixed with **DBNHC** at a molar ratio 1:4. Then, this mixed solution was further spiked with different amounts of warfarin or ibuprofen and the resultant ternary mixtures were subjected for the fluorescence measurement.

Steady-state Fluorescence Anisotropy

Fluorescence anisotropy (r) measurements were carried out by considering the following equation described by Larsson *et al.* ¹

$$r = \frac{I_{VV} - GI_{VH}}{I_{VV} + 2GI_{VH}} \quad (\text{Eq. S1})$$

Where, the polarizer positions were set at $(0^\circ, 0^\circ)$, $(0^\circ, 90^\circ)$, $(90^\circ, 0^\circ)$, and $(90^\circ, 90^\circ)$ to get, I_{VV} , I_{VH} , I_{HV} , I_{HH} for excitation and emission signals respectively. G factor is defined as

$$G = \frac{I_{HV}}{I_{HH}} \quad (\text{Eq. S2})$$

Where, I_{HV} and I_{HH} are respectively the vertical and horizontal component of emission polarizer, keeping the excitation polarizer horizontal. G depends on slit widths and monochromator wavelength. The excitation and emission wavelengths were fixed at 355nm and 450 nm respectively.

Fluorescence Lifetime Studies

The TCSPC measurements were carried out in 10 mM PBS buffer solution of pH 7.4 for the fluorescence decay of **DBNHC** in the absence and presence of increasing concentration of BSA at 25 $^\circ$ C. During the TCSPC measurements the photoexcitation was fixed at 355 nm. Here, sodium dodecyl sulfate is used as the IRF of the exciting source in the TCSPC measurement. The fluorescence decay curves were fitted to a biexponential function:

$$I(t) = A + \alpha_1 \cdot e^{(-t/\tau_1)} + \alpha_2 \cdot e^{(-t/\tau_2)} \quad (\text{Eq. S3})$$

SUPPORTING FILE

Where, α_i represents the i th pre-exponential factor and τ_i denotes the decay time of component i (here $i = 1, 2$). The average lifetimes (τ_{avg}) for the fluorescence decay profiles were calculated by using the following equation:²

$$\tau_{avg} = \sum_{i=1}^2 \alpha_i \cdot \tau_i / \alpha_i \quad (\text{Eq. S4})$$

Fluorescence Quantum Yield Measurements

Fluorescence quantum yield were calculated by adopting the reported strategy³ where relative measurement was carried out using Quinine sulphate as reference ($\Phi_s = 0.546$ in H_2SO_4) and by considering the following equation:

$$\Phi_u = \frac{A_s F_u \eta_u^2}{A_u F_s \eta_s^2} \times \Phi_s \quad (\text{Eq. S5})$$

Where, " Φ " is the quantum yield; " A " is the optical density; " F " is the measured integrated emission intensity; and " η " is the refractive index. The subscript " u " refers to the unknown sample, and subscript " s " refers to the standard reference with a known quantum yield.

Detection limit

The detection limit was calculated on the basis of the fluorescence titration with BSA. The standard deviation, σ , of the blank (**DBNHC** only) was determined by measuring the fluorescence intensity 10 times separately at a fixed concentration of 5 μM . Then, the fluorescence emission at 450 nm was plotted as a function of the concentration of BSA from the corresponding titration experiment to evaluate the slope. The detection limit was then calculated using the following equation:⁴

$$\text{Detection limit} = 3\sigma/k \quad (\text{Eq. S6})$$

Where " σ " is the standard deviation of blank measurement, and " k " is the slope between the fluorescence emission intensity versus [BSA].

Dynamic Light Scattering Studies

The particle sizes of **DBNHC** and the aggregates of **DBNHC** with 1 equiv. of BSA were measured by dynamic light scattering (DLS) measurements at 25 °C on a Malvern Zetasizer Nano ZS instrument. At first, DLS measurement was performed with 5 μM **DBNHC** in PBS buffer solution (pH 7.4). Then, to determine the change in particle size of **DBNHC** upon interaction with BSA, a DLS study was also performed with of 5 μM **DBNHC** in the presence of 2 equiv. BSA in PBS buffer solution (pH 7.4).

Transmission Electron Microscopy (TEM) Analysis

The morphology of **DBNHC** (5 μM) and the aggregates of **DBNHC** (5 μM) with 2 equiv. BSA in PBS buffer solution (pH 7.4) were characterized in a 2100 Plus Electron Microscope of 200 kV TEM instrument by drop casting of the sample separately on carbon-coated copper grids (300 meshes) and drying them in a vacuum.

Molecular Docking Study

To know the probable binding sites within BSA and the binding mode of **DBNHC** with BSA, molecular docking study was performed using docking program AutoDock (version 4.2). The X-ray crystal structure of BSA was taken from RCSB Protein Data Bank having PDB ID: 4F5S. To draw the structure of **DBNHC**, Chem3D Ultra 12.0 was used and further modification was carried out by using Gaussian 09W and AutoDock 4.2 programs. Gasteiger charges and polar hydrogen atoms were added to the protein and probe. Grid box with dimensions of 110 Å × 110 Å × 110 Å and 0.403 Å grid spacing were specified to enclose the protein using AutoGrid program. The default values shown by the AutoDock program were used for other sets of parameters. The Lamarckian genetic algorithm (LGA) was used to accomplish docking calculations and the grid maps for energy were calculated by AutoGrid.^{5,6} The best optimized docked model with lowest binding energy was considered for further study of docking simulations and the output was best viewed by using Discovery Studio.

Cell Cytotoxicity Assay and fluorescence analysis

SUPPORTING FILE

A549 cell line were cultured in DMEM+10% FBS supplemented with antibiotics (penicillin-100 µg/ml; streptomycin-50 µg/ml) at 37°C in 95% air, 5% CO₂ incubator. A549 cells were seed in 96-well plate at 37°C and exposed to varying concentrations of DBNHC range between 10-50 µM 24 hr. Cell Viability was performed by using MTT assay as per manufactures protocol. The cell viability (%) was expressed as a percentage compared to the untreated control cells. A549 cells were seeded on cover slip place in 35x10 mm culture dish for 24h at 37°C. The A549 cells were allowed to incubate with 5 µM of DBNHC for 30 min, preincubated 20 and 40 µM BSA for 2 hour followed with 5 uM DBNHC at 37°C for 30 min. After incubation, cells were washed thrice with 1X PBS and mounted for visualization. Bright field and fluorescence images of A549 cells were taken by fluorescence microscope (Leica DM3000, Germany) with an objective lens of 40X magnification.

References

- 1) A. Larsson, C. Carlsson, M. Jonsson, B. Albinsson, *J. Am. Chem. Soc.* 1994, **116**, 8459–8465.
- 2) M. Sasmal, R. Bhowmick, A. S. M. Islam, S. Bhuiya, S. Das, M. Ali, *ACS Omega* 2018, **3**, 6293–6304.
- 3) A. M. Brouwer, *Pure Appl. Chem.* 2011, **83**, 2213–2228.
- 4) T. Zhu, J. Du, W. Cao, J. Fan, X. Peng, *Ind. Eng. Chem. Res.* 2016, **55**, 527–533.
- 5) G. M. Morris, D. S. Goodsell, R. Huey, A. J. Olson, Distributed Automated Docking of Flexible Ligands to Proteins: Parallel Applications of AutoDock 2.4. *J. Comput.-Aided Mol. Des.* 1996, **10**, 293–304.
- 6) G. M. Morris, D. S. Goodsell, R. S. Halliday, R. Huey, W. E. Hart, R. K. Belew, A. J. Olson, Automated Docking Using a Lamarckian Genetic Algorithm and Empirical Binding Free Energy Function. *J. Comput. Chem.* 1998, **19**, 1639–1662.